A kernelized fuzzy c-means algorithm for automatic magnetic resonance image segmentation

E.A. Zanaty[a], Sultan Aljahdali[a,*] and Narayan Debnath[b]
[a]*College of Computer Science, Taif University, Taif, Saudi Arabia*
[b]*Computer Science Department, Winona State University, Winona, MN 55987, USA*

Abstract. In this paper, we present alternative Kernelized FCM algorithms (KFCM) that could improve magnetic resonance imaging (MRI) segmentation. Then we implement the proposed KFCM method with considering some spatial constraints on the objective function. The algorithms incorporate spatial information into the membership function and the validity procedure for clustering. We use the intra-cluster distance measure, which is simply the median distance between a point and its cluster centre. The number of the cluster increases automatically according the value of intra-cluster, for example when a cluster is obtained, it uses this cluster to evaluate intra-cluster of the next cluster as input to the KFCM and so on, stop only when intra-cluster is smaller than a prescribe value. The most important aspect of the proposed algorithms is actually to work automatically. Alterative is to improve automatic image segmentation.

These methods are applied on two different sets: reference images, for objective evaluation based on estimation of segmentation accuracy and time, and non reference images, for objective evaluation based on combined judgment of opinions of specialists.

Keywords: Medical imaging, fuzzy clustering, image segmentation

1. Introduction

Magnetic resonance imaging (MRI) provides information about the human soft tissue anatomy [1]. It reveals fine details of anatomy, and yet is noninvasive and does not require ionizing radiation such as x-rays. It is a highly flexible technique where contrast between one tissue and another in an image can be varied simply by varying the way the image is made. For example, by altering radio-frequency (RF) and gradient pulses, and by carefully choosing relaxation timings, it is possible to highlight different components in the object being imaged and produce high contrast images. The rich anatomy information provided by MRI has made it an indispensable tool for medical diagnosis in recent years In particular, as a task of delineating anatomical structures and other regions of interest, image segmentation algorithms play a vital role in numerous biomedical imaging applications such as the quantification of tissue volumes, diagnosis, study of anatomical structure, and computer-integrated surgery [1–3]. Classically, image segmentation is defined as the partitioning of an image into nonoverlapping, constituent regions which are homogeneous with respect to some characteristics such as intensity or texture.

---

*Corresponding author. E-mail: aljahdali@tu.edu.sa.

Because of the advantages of magnetic resonance imaging (MRI) over other diagnostic imaging [2], the majority of researches in medical image segmentation pertains to its use for MR images, and there are a lot of methods available for MR image segmentation [2–6]. Among them, fuzzy segmentation methods are of considerable benefits, because they could retain much more information from the original image than hard segmentation methods [3]. In particular, the fuzzy C-means (FCM) algorithm [7], assign pixels to fuzzy clusters without labels. Unlike the hard clustering methods which force pixels to belong exclusively to one class, FCM allows pixels to belong to multiple clusters with varying degrees of membership. Because of the additional flexibility, FCM has been widely used in MR image segmentation applications recently. However, because of the spatial intensity inhomogeneity induced by the radio-frequency coil in MR image, conventional intensity-based FCM algorithm has proven to be problematic, even when advanced techniques such as non-parametric, multi-channel methods are used [2]. To deal with the inhomogeneity problem, many algorithms have been proposed by adding correction steps before segmenting the image [4,5] or by modeling the image as the product of the original image and a smooth varying multiplier field [2,6]. Recently, many researchers have incorporated spatial information into the original FCM algorithm to better segment the images [6,8–10]. Tolias and Panas [8] proposed a fuzzy rule-based system to impose spatial continuity on FCM, and in another paper [9], they used a small positive constant to modify the membership of the center pixel in a 3×3 window. Pham et al. [6] modified the objective function in the FCM algorithm to include a multiplier field containing the first- and second-order information of the image. Similarly, Ahmed et al. [11] proposed an algorithm to compensate for the intensity inhomogeneity and to label a pixel by considering its immediate neighborhood. A rather recent approach proposed by Pham [12] is to penalize the FCM objective function to constrain the behavior of the membership functions, similar to methods used in the regularization and Markov random field (MRF) theory.

The FCM algorithm often uses a Euclidean distance measure, which is fine for most noise-free data. However difficulties arise when data is corrupted by noise or outliers. In order to deal with these kinds of data sets, kernel methods have been widely applied. The fundamental idea of kernel methods is to transform the original low-dimensional input space into a higher dimensional feature space through some (nonlinear) mapping, therefore some complex linear problems in the original space can possibly be solved in the transformed highdimensional space. The kernelized FCM (KFCM) [13–16] used a kernel function as a substitute for the inner product in the original space, which is like mapping the space into higher dimensional feature space [13]. The objective function for FCM then has a new form. There have been a number of other approaches to incorporating kernels into fuzzy clustering algorithms. These include enhancing clustering algorithms designed to handle different shape clusters [16]. An approach which is designed for incomplete data [15] and a different formulation of a centroid-based clustering algorithm [14]. More recent results of fuzzy algorithms have been presented in [17] for improving automatic MRI image segmentation. They use the intra-cluster distance measure to give the ideal number of clusters automatically, more discussion can be shown in [17].

Although most fuzzy methods have several advantages such as: (1) it yields regions more homogeneous than those of other methods, (2) it reduces the spurious blobs, (3) it removes noisy spots, and (4) it is less sensitive to noise than other techniques. The final number of clusters is still always sensitive to one or two user-selected parameters that define the threshold criterion for merging. Though some compatibility or similarity measure are applied to choose the clusters to be merged, no validity measure is used to guarantee that the clustering result after a merge is better than the one before the merge. Partial results were stated in [18] to answer the questions: "Can the appropriate number of clusters be determined automatically? And if the answer is yes, how?". The number of clusters is determined by operating

index procedures to whole data to determine the number of clusters before starting fuzzy methods. This will consume much time for finding the suitable number of cluster. Therefore, two major problems are known with fuzzy methods: (1) How to determine the number of clusters. (2) The computational cost is quit high for large data sets.

This paper addresses these problems for overcoming the shortcomings of existing fuzzy methods. We present alternative Kernlized FCM algorithms (KFCM) that could improve MRI segmentation. Then we implement the proposed KFCM method with considering some spatial constraints on the objective function. Our algorithms are an extension of the results carried by [17] for investigating automatic MRI segmentation. Since the KFCM method aims to minimize the sum of squared distances from all points to their cluster centers, this should result in compact clusters. Therefore the distance of the points from their cluster centre is used to determine whether the clusters are compact. For this purpose, we use the intra-cluster distance measure, which is simply the median distance between a point and its cluster centre. The intra-cluster is used to give us the ideal number of clusters automatically; i.e. a centre of the first cluster is used to estimate the second cluster, while an intra-cluster of the second cluster is obtained. Similarly, the third cluster is estimated using the centre and intra cluster of the second cluster, so on, and only stop when the intra-cluster is smaller than a prescribed value.

The suggested algorithms are evaluated and compared with established KFCM and with spatial constrained methods by applying them on simulated volumetric MRI and real MRI data to prove their efficiency. The application of these algorithms to a real MRI dataset cannot give us a quantitative measure about how much successful they are. As such, the segmentation results are judged visually by specialists.

The rest of this paper is organized as follows: Section 2 describes the MRI segmentation problem. The proposed KFCM clustring algorithm and SKFCM are presented in Sections 3, 4 respectively. Experimental comparisons are given in Section 5. Finally, Section 6 gives our conclusions.

2. The MRI segmentation problem

The basic idea of image segmentation can be described as follows. Given a set of data $X = \{x_1, x_2, \ldots, x_N\}$ and a uniformity predicate P, we wish to obtain a partition of the data into disjoint nonempty groups $X = \{v_1, v_2, \ldots, v_k\}$ subject to the following conditions:

1. $\cup_{i=1}^{k} v_i = X$
2. $v_i \cap v_j = \phi, i \neq j$
3. $P(vi) = \text{TRUE}, i = 1, 2, \ldots, k$
4. $P(vi \cup vj) = \text{FALSE}, i \neq j$

The first condition ensures that every data value must be assigned to a group, while the second condition ensures that a data value can be assigned to only one group. The third and fourth conditions imply that every data value in one group must satisfy the uniformity predicate while data values from two different groups must fail the uniformity criterion.

To obtain a 3D MR image, the positional information about the tissues must be recorded. This involves isolating the source of each component of the MR signal to a particular voxel using the technique of spatial encoding. In MR imaging, spatial encoding is achieved by performing slice selection in one direction (e.g. the z-axis), frequency encoding in another direction (e.g. the x-axis), and phase encoding in the third direction (e.g. the y-axis). In slice selection, a narrow bandwidth is applied in the presence of a z-axis linear gradient field. Since the resonance frequency of a proton is proportional to the applied

magnetic field, the presence of a gradient field means that only a narrow slice in the body will have a resonant frequency within the bandwidth of the resonant frequency [19–21].

MR image segmentation involves the seperation of image pixels into regions comprising different tissue type. All MR images are affected by random noise. The noise comes from the stray current in the detector coil due to the fluctuating magnetic fields arising from random ionic currents in the body, or the thermal fluctuations in the detector coil itself, more discussion can be seen [19]. When the level of noise is significant in an MR image, tissues that are similar in contrast could not be delineated effectively, causing error in tissue segmentation. Then more sophisticated techniques would be needed to reconstruct the image from incomplete information [22,23]. A 3D image can be obtained from many consecutive 2D slices.

3. The proposed Kernelized fuzzy c-means method (KFCM)

The kernel methods [24] are one of the most researched subjects within machine learning community in the recent few years and have widely been applied to pattern recognition and function approximation. The main motives of using the kernel methods consist of: (1) inducing a class of robust non-Euclidean distance measures for the original data space to derive new objective functions and thus clustering the non-Euclidean structures in data; (2) enhancing robustness of the original clustering algorithms to noise and outliers, and (3) still retaining computational simplicity.

The algorithm is realized by modifying the objective function in the conventional fuzzy c-means (FCM) algorithm using a kernel-induced distance instead of Euclidean distance in the FCM, and thus the corresponding algorithm is derived and called as the kernelized fuzzy c-means (KFCM) algorithm, which to be more robust than FCM.

In FCM, the membership matrix U is allowed to have not only 0 and 1 but also the elements with any values between 0 and 1, this matrix satisfies the constraints:

$$\sum_{i=1}^{C} u_{ij} = 1, \forall j = 1, \ldots, N \tag{1}$$

In this work, the kernel function $K(x, C)$ is taken as the Gaussian radial basic function (GRBF):

$$K(x, c) = \exp\left(\frac{-\|x - c\|^2}{\sigma^2}\right), \tag{2}$$

where σ is an adjustable parameter. The objective function is given by:

$$j_m = 2 \sum_{i=1}^{C} \sum_{j=1}^{N} u_{ij}^m (1 - K(x_j, c_i)). \tag{3}$$

The fuzzy membership matrix u can be obtained from:

$$u_{ij} = \frac{(1 - K(x_j, c_i))^{-1/(m-1)}}{\sum_{k=1}^{C} (1 - K(x_j, c_k))^{-1/(m-1)}}. \tag{4}$$

The cluster center c_i can be obtained from:

$$c_i = \frac{\sum_{j=1}^{N} u_{ij}^m K(x_j, c_i) x_j}{\sum_{j=1}^{N} u_{ij}^m K(x_j, c_i)}. \tag{5}$$

Since the K-means method aims to minimize the sum of squared distances from all points to their cluster centers, this should result in compact clusters. We use the intra-cluster distance measure, which is simply the median distance between a point and its cluster centre. The equation is given as:

$$\text{intra} = \text{midean} \left(\sum_{i=1}^{C} \sum_{x \in c_i} \|x - v_i\|^2 \right) \tag{6}$$

Therefore, the clustering which gives a minimum value for the validity measure will tell us what the ideal value of the clusters. Then the number of cluster is known before estimating the membership matrix.

The proposed KFCM clustering algorithm is composed of the following steps:

Step 1: Select a subset from the dataset and initialize the cluster centers $c_i, i = 1, \ldots, C$..

Step 2: $C = 2$ the initial number of cluster, $C_{\max}$ = the maximum number of cluster, it is seleced arbitrary.

Step 3: Initialize the membership matrix U with random values between 0 and 1 such that the constraints in Eq. (1) are satisfied.

Step 4: Calculate fuzzy cluster centers $c_i, i = 1, \ldots, C$ using Eq. (5).

Step 5: Compute the cost function (objective function) according to Eq. (3). Goto step 9, if either it is below a certain tolerance value or its improvement over previous iteration is below a certain threshold.

Step 6: Compute a new membership matrix U using Eq. (4).

Step 7: Obtain center C_1.

Step 8: Goto step3 on the subset with c number of cluster to obtain center C_2.

Step 9: Use C_2 to calculate the intra distance according to the above Eq. (6), stop if intra is smaller than a prescribe value.

Step 10: $C = C + 1$, return to step 3, until $C = Cmax$

Step 11: Stop.

4. The proposed spatial constrained SKFCM method

SKFCM is applied directy to image segmentation like KFCM, it would be helpful to consider some spatial constraints on the objective function. This penalty term contains spatial neighborhood information, which acts as a regularizer and biases the solution toward piecewise-homogeneous labeling. Such regualization is helpful in segmenting images corrupted by noise. The objective function is as follows:

$$j_m = \sum_{i=1}^{C} \sum_{j=1}^{N} u_{ij}^m \left(1 - K(x_j, c_i)\right) + \frac{\alpha}{N_R} \sum_{i=1}^{C} \sum_{j=1}^{N} u_{ij}^m \sum_{r \in N_j} (1 - u_{ir})^m \tag{7}$$

where N_j stands for the set of neighbors that exist in a window around x_j (do not include x_j itself) and N_R is the cardinality of N_j. The parameter α controls the effect of the penalty term and lies between zero and one inclusive.

<table>
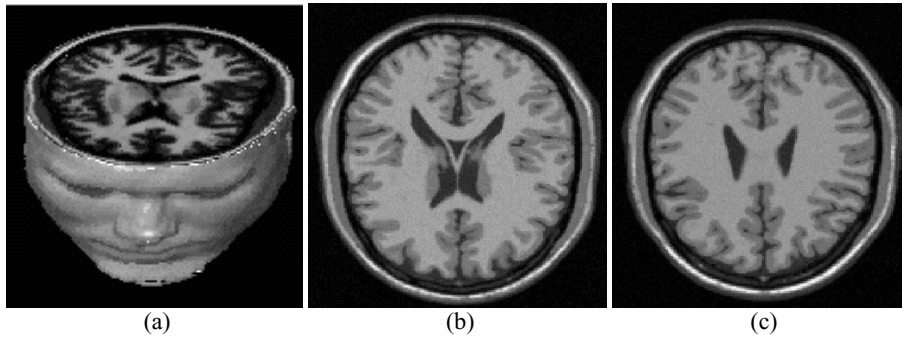<tr><td>(a)</td><td>(b)</td><td>(c)</td></tr>
</table>

Fig. 1. Test images: a) 3D simulated data, b) and c) two original slices from the 3D simulated data (slice91, and slice100).

An iterative algorithm for minimizing Eq. (12) is derived by evaluating the centroids and membership functions that satisfy a zero gradient condition like the KFCM. A necessary condition on uij for Eq. (12) to be at a local minimum or a saddle point is:

$$u_{ij} = \frac{\left((1 - K(x_j, c_i)) + \left(\alpha \sum_{r \in N_j} (1 - u_{ir})^m / N_R \right) \right)^{-1/(m-1)}}{\sum_{k=1}^{C} \left((1 - K(x_j, c_k)) + \left(\alpha \sum_{r \in N_j} (1 - u_{kr})^m / N_R \right) \right)^{-1/(m-1)}}. \tag{8}$$

The proposed SKFCM algorithm is almost identical to the KFCM, except in Step 4, Eq. (8) is used instead of Eq. (4) to update the memberships.

5. Experimental and comparative results

The experiments were performed with several data sets on a PC with a P4 2.4 GHZ CPU, 256 MB of RAM and performed in MATLAB. Our expremint includes simulated volumetric MR data consisting of several classes. The experiments were performed with several data sets on a PC with a P4 2.4 GHZ CPU, 256 MB of RAM and performed in MATLAB. The advantages of using digital phantoms rather than real image data for validating segmentation methods include prior knowledge of the true tissue types and control over image parameters such as modality, slice thickness, noise and intensity inhomogeneities. We used a high-resolution T1-weighted MR phantom with slice thickness of 1 mm, 3% noise and no intensity inhomogeneities, obtained from the classical simulated brain database of McGill University [25]. Two transverse slices drawn from the simulated MR data are shown in Fig. (1d), (1e), and (1f). MRI has several advantages over other imaging techniques enabling it to provide 3-dimensional data with high contrast between soft tissues (see Fig. (1c)). However, the amount of data is far too much for manual analysis/interpretation, and this has been one of the biggest obstacles in the effective use of MRI. Segmentation of MR images into different tissue classes, especially gray matter (GM), white matter (WM) and cerebrospinal fluid (CSF), is an important task. Brain MR images have a number of features, especially the following: Firstly, they are statistically simple: MR Images are theoretically piecewise constant with a small number of classes. Secondly, they can have relatively high contrast between different tissues. Unlike many other medical imaging modalities, the contrast in an MR image depends strongly upon the way the image is acquired.
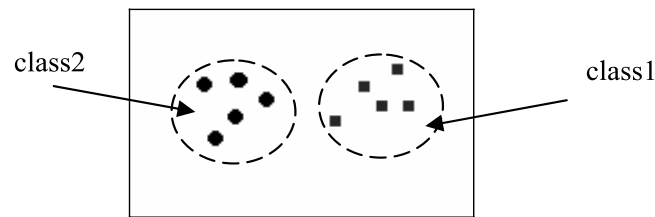
Fig. 2. Two accuracy measure evaluated on a two-class example.

The quality of the segmentation algorithm is of vital importance to the segmentation process. The comparison score S for each algorithm is proposed in [25], which defined as:

$$S = \left| \frac{A \cap A_{ref}}{A \cup A_{ref}} \right| \tag{9}$$

where A represents the set of pixels belonging to a class as found by a particular method and A_{ref} represents the set of pixels belonging to the very same class in the reference segmented image (ground truth).

Another accuracy measure, segmentation accuracy (overall accuracy) S' is computed by dividing the total number of correct number of correct classified pixels over the total number of pixels [26].

The measure S is more conservative than S' in evaluating the segmentation quality as shown in the following example. Assume we have a simple synthetic data set with 10 pixels, which is plotted in Fig. 2, and contains two classes, with 5 pixels in each class. Assume the segmentation method is applied to these dataset, where the segmentation results gives 6 pixels in class1 and 4 pixels in class2. The two measures will yield $S = 9/11$, $S' = 9/10$. The value of S is lower as it penalizes the misclassification of the pixels more. Thus we will use S in our experiments.

5.1. KFCM and SKFCM results

Here we compare the evaluation of our proposed methods to the standard kernelized fuzzy c-means (KFCM) and spatial constrained KFCM methods. Which is the Gaussian RBF kernel is used for KFCM and SKFCM. We set the parameters $m = 2$, $\sigma = 150$, $\alpha = 0.7$ and $N_R = 26$ when using 3D MR phantom image, because the added noise is relatively big, otherwise we use $\alpha = 0.1$, and $N_R = 8$ (a 3×3 window centered around each pixel). These values will be used in the rest of this work if no specific value is explicitly stated.

5.1.1. In the Case of determining the true cluster

We experiment the propsed KFCM and SKFCM with different level of noise (simulated volumetric MR data). They are tested for determining the number of cluster automatically. We used a high-resolution T1-weighted MR phantom with slice thickness of 1 mm, 3% noise and no intensity inhomogeneities, obtained from the classical simulated brain database of McGill University [25]. The Figs 3 and 4 describe the relation between the noise points (XB) and the number of clusters. For the propsed SKFCM as the level noise increase, the obtained number of clusters increases. The propsed KFCM shows constant and inconsistent behavior on the sets of classes. The both methods are sensetive to noise, i.e. with low number of noise, they get 10 clusters (true segments), and the results are varied according to noise factor, although SKFCM gives correct result with high noise points as in fourth and fifth charts in Fig. 4.

S130   *E.A. Zanaty et al. / A kernelized fuzzy c-means algorithm for automatic magnetic resonance image segmentation*
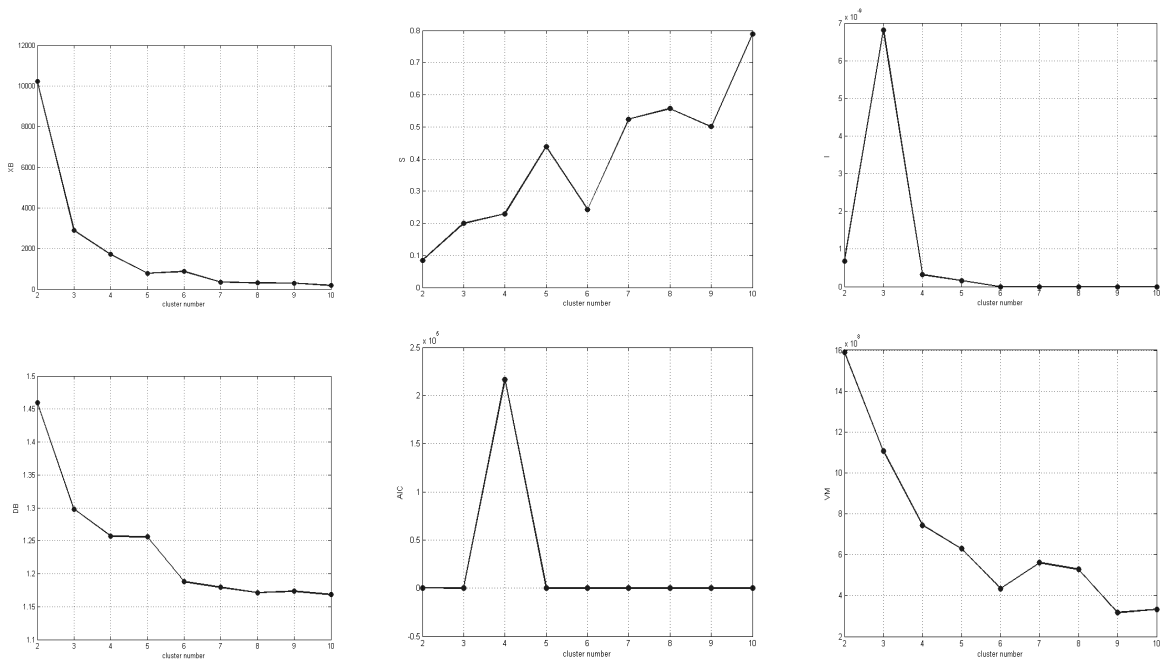

Fig. 3. Variation of the different noise level with the number of clusters for 3D MRI using KFCM algorithm.
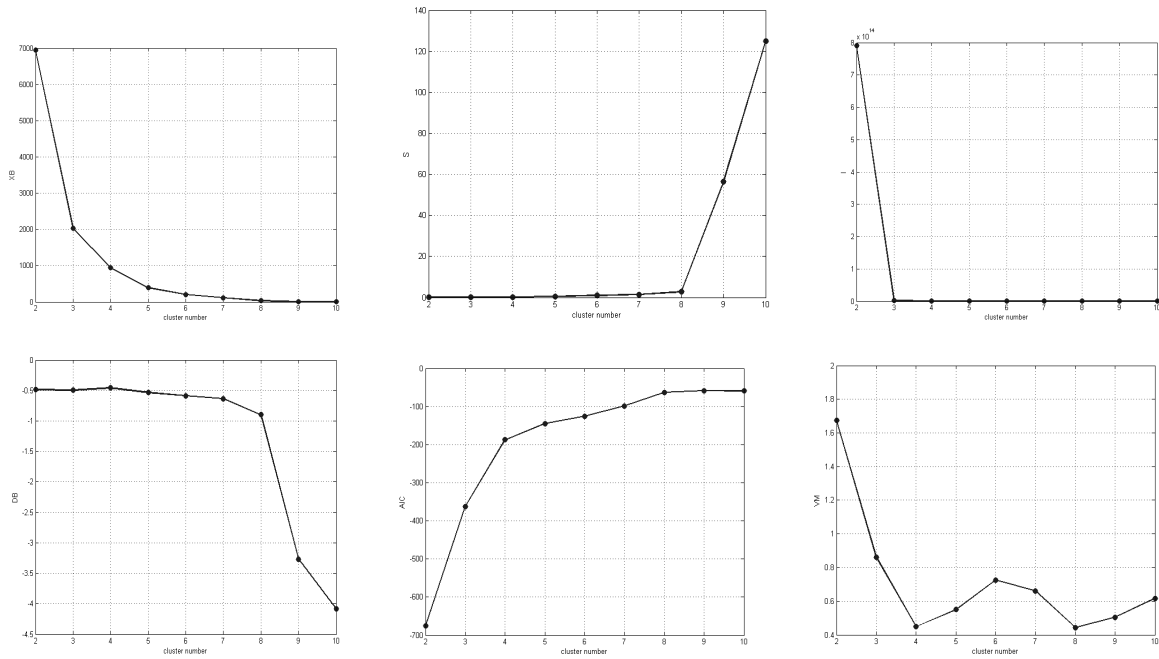

Fig. 4. Variation of the different noise level with the number of clusters for 3D MRI using SKFCM algorithm.

Table 1
Segmentation accuracy of individual
methods on MRI volume dataset

Methods	Accuracy MRI volume
KFCM	0.51432
SKFCM	0.52543
The proposed KFCM	0.54708
The proposed SKFCM	0.55394

Table 2
Segmentation accuracy (%) of eight methods on real brain classes

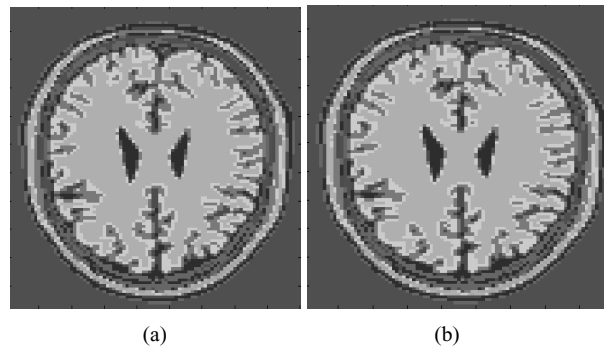|	Class1	Class2	Class3	Class4	Class5	Class6	Class7	Class8	Class9	Over all
KFCM	67.55	51.14	58.83	100.0	67.96	21.87	59.21	11.27	97.26	59.454
SKFCM	75.46	71.88	99.98	100.0	96.63	82.31	55.70	1.50	96.82	75.58
The proposed KFCM	66.87	55.77	59.087	100.0	70.32	37.96	63.99	10.12	97.99	62.456
The proposed SKFCM	79.54	77.55	98.34	100.0	98.65	81.98	55.70	9.54	99.54	77.87

(a)　　　　　　　(b)

Fig. 5. Segmentation results for the slice ($z = 100$) on a simulated data using methods: (a) KFCM, (b) SKFCM.

5.1.2. Experiments on the phantom image

Table 1 shows the corresponding average percentage of accuracy scores of the individual segmentation methods, after applying them to the simulated MR data (three slices of the segmented 3D MR volume). The advantages for using digital phantoms rather than real image data for validating segmentation methods include prior knowledge of the true tissue types and control over image parameters such as modality, slice thickness, noise and intensity inhomogeneities. The volume was reduced in size to $181 \times 108 \times 90$ to reduce the high computational cost. A qualitative representation of the segmentation results is shown in Figs 5, 6 and 7. The figures show three slices of the segmented 3D MR volume.

5.1.3. Experiment on the real MR data

Table 2 shows the corresponding accuracy scores of the eight methods for the nine classes of real images (real brain image with nine classes. Obviously, the proposed SKFCM acquires the best segmentation performance. After that, the proposed KFCM, and then the established SKFCM and KFCM. The proposed KFCM and SKFCM methods still more stable and achieve much better performance than the others for different classes.

Table 3
Comparisons of running time of eight algorithms on synthetic, phantom, and real images (seconds)

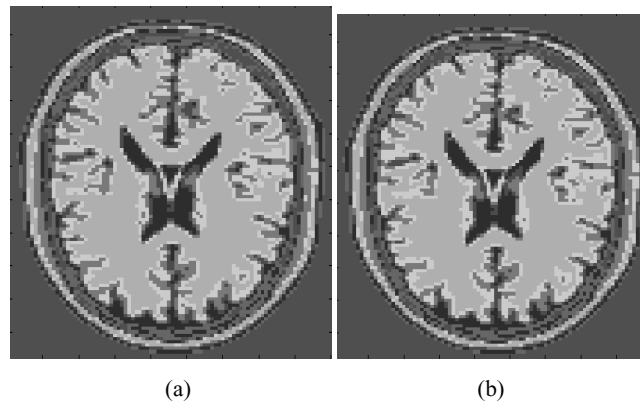|	KFCM	The proposed KFCM	SKFCM	The proposed SKFCM
Phantom image	108.883	154.87	286.98	20.654
Real image	285.98	100.876	1.765e+003	2.654e+003

(a) (b)

Fig. 6. Segmentation results for the slice ($z = 91$) on a simulated data using methods: (a) KFCM, (b) SKFCM.
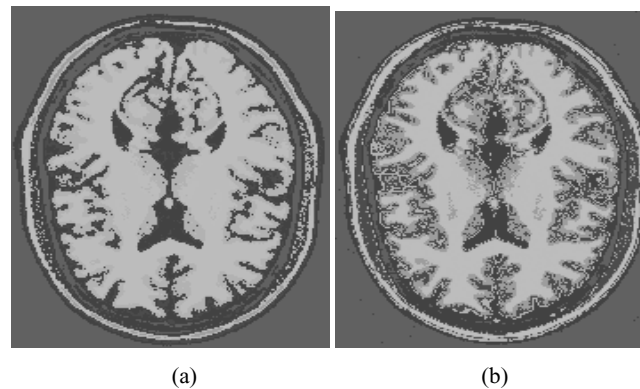

(a) (b)

Fig. 7. Segmentation results on a simulated brain MR brain image. (a) KFCM, (b) SKFCM.

5.1.4. Time overhead

Table 3 shows the comparison of the CPU time for the three test images, synthetic, simulated MR images, real MR images. These times have been computed from the time average of all given images that have same type. For example, the time of phantom image 108.883 is obtained by computing the average of nine classes times. From this table, the established KFCM and SKFCM are faster than the proposed methods for all tested data sets, due to the proposed methods consume much time for obtaining the true number of segments. This costs are acceptable for achieving more accurate and automatic MRI segmentation.

Table 4
The rank of data1 and data2

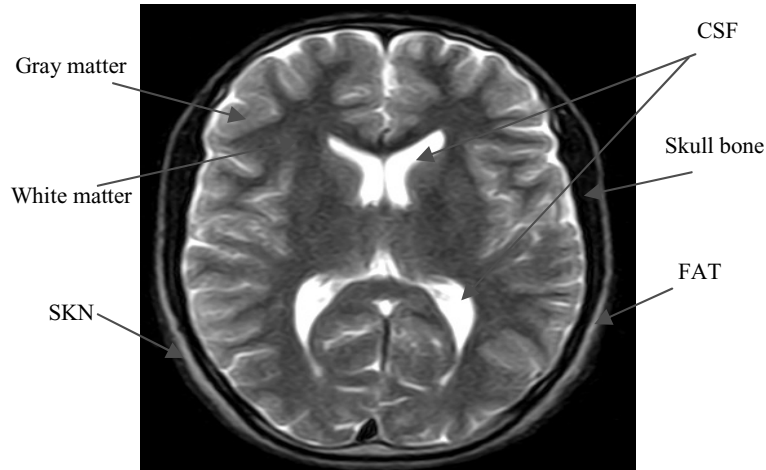|	Methods	Rank data1	Rank data2	Rank total
Individual methods	KFCM	3	4	3
	SKFCM	2	3	2
	The proposed KFCM	2	2	2
	The proposed SKFCM	2	1	1

Fig. 8. The anatomical model for real MRI image.

5.2. Specialists judgment

In this section, two real T2-weigthed MRI images (data1 and data2) are obtained as test sets from the x-ray Department, Faculty of Medicine as shown in Figs (9a), (9c). The anatomical model used to generate real brain MRI data consist of tissue volumes, one for each tissue class (white mater (WM) within the brain parenchyma, gray matter (GM) within the brain parenchyma, cerebro spinal fluid (CSF) surrounding the brain and within the ventricles, fatty tissue (FAT), Skull bone (does not include sinuses), SKN (mostly skin)). The voxel values in these volumes reflects the proportion of tissue presented in the voxel, in the range [0,255] as shown in Fig. 8.

We take the opinion of five medical doctors in PhD degree. They have some knowledge about number of clusters in the images, where the number of clusters in algorithms are determined beforehand. Which each slice with six classes and consisting of 384×512 pixels. Qualitative representation of the segmentation results for two real MRI image are shown in Figs (10), (11), using the segmentation methods. The application of these algorithms to a real MRI dataset cannot give us a quantitative measure about how they are successful. As such, qualitative assessment of the segmentation results is judged visually.

We present qualitative comparison results of the segmented image methods, where the opinion of doctors from x-ray department has been considered. In case data2, all of them show that the proposed KFCM and SKFCM methods give better results, as shown in Table 4 which a value/reference of one is the best and six is the worst method. After that, the standard SKFCM method respectively misclassified some parts of gray matter into white matter.

On the other hand, data1 more complicated than data2, so the judge on this data become more difficult. In this case, all doctors shows that the proposed KFCM and SKFCM segmentation methods give better
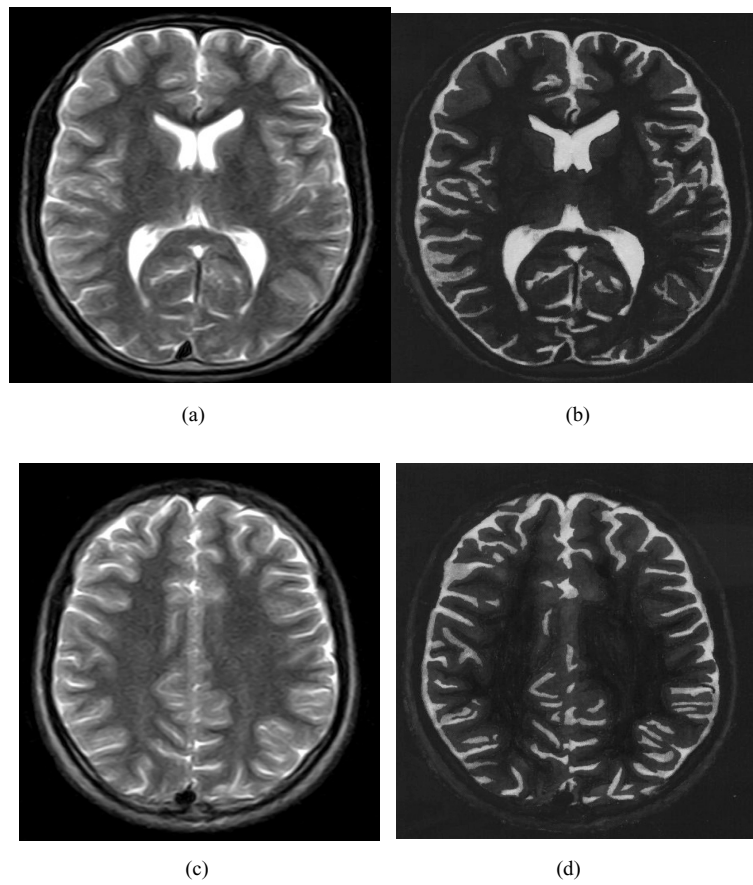
(a)   (b)

(c)   (d)

Fig. 9. MRI image. a) Original image of data1 image, b) manual segmentation of the image shown in (14a), c) Original image of data2 image and d) manual segmentation of the image shown in (14c).
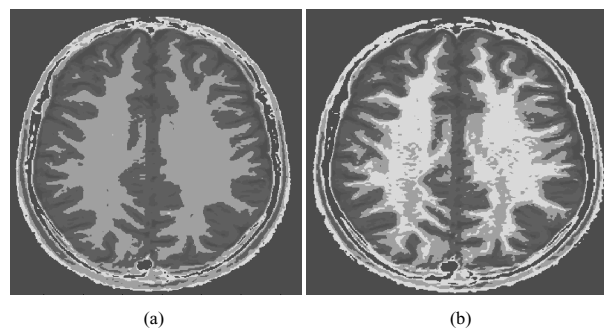

(a)   (b)

Fig. 10. Segmentation of real MRI image (data2): a) KFCM, b) SKFCM.

results. After that, SKFCM method misclassified most parts of gray matter into white matter. In contrast, the standard KFCM method can yield satisfactory result, which is more compatible with human visual perception.

We rearrange the reference according to majority of doctors after seeing the different results as shown
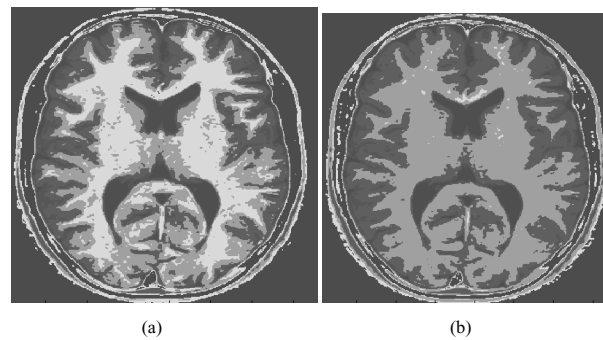
(a)   (b)

Fig. 11. Segmentation of real MRI image (data1): a) KFCM, b) SKFCM.

in Table 4, which the rank total is computed through computed the average percentage between the two data when using one method. The percentage is assumed, which reference 1, 2, ..., 6 take percentage 60, 50, ..., 10 respectively.

6. Conclusion

The results of the proposed KFCM and SKFCM segmentation methods have been presented. Rather than tuning a method for the best possible performance, it works automatically and can indeed improve the segmentation accuracy over the existing methods. The algorithms incorporate spatial information into the membership function and the validity procedure for clustering. They have estimated accurate clusters automatically even without prior knowledge of the true tissue types and the number of cluster of given images. Extensive experiments using MR images generated by the BrainWeb simulator [15] and real MR data have been used to evaluate the proposed methods. Due to the use of soft segmentation, the proposed FCM algorithm is able to give a good estimation of tissue volume in the presence of inaccurate tissues. It is observed that the proposed methods have shown higher robustness in discrimination of regions because of the low signal/noise ratio characterising most of medical images data.

By comparing the proposed methods with established one, it is clear that our algorithms can estimate the correct tissues much more accurately than the established algorithms. Although, the number of clusters are varied according to noise factor, but we have shown that the proposed SKFCM gives a correct number of clusters with high noise level. In other hand, the established KFCM and SKFCM are much faster than the proposed methods for all tested data sets, due the proposed methods consume much time for obtaining the true number of segments. This costs are acceptable for achieving more accurate and automatic MRI segmentation.

Future research in MRI segmentation should strive toward improving the accuracy, precision, and computation speed of the segmentation algorithms, while reducing the amount of manual interactions needed. This is particularly important as MR imaging is becoming a routine diagnostic procedure in clinical practice. It is also important that any practical segmentation algorithm should deal with 3D volume segmentation instead of 2D slice by slice segmentation, since MRI data is 3D in nature.

References

[1] D.L. Pham, C.Y. Xu and J.L. Prince, A survey of current methods in medical image segmentation, *Ann Rev Biomed Eng* **2** (2000), 315–337 [Technical report version, JHU/ECE 99-101, Johns Hopkins University].

[2] W.M. Wells, W.E.L. Grimson, R. Kikinis and S.R. Arrdrige, Adaptive segmentation of MRI data, *IEEE Trans Med Imaging* **15** (1996), 429–442.

[3] J.C. Bezdek, L.O. Hall and L.P. Clarke, Review of MR image segmentation techniques using pattern recognition, *Med Phys* **20** (1993), 1033–1048.

[4] B.M. Dawant, A.P. Zijidenbos and R.A. Margolin, Correction of intensity variations in MR image for computer-aided tissue classification, *IEEE Trans Med Imaging* **12** (1993), 770–781.

[5] B. Johnson, M.S. Atkins, B. Mackiewich and M. Andson, Segmentation of multiple sclerosis lesions in intensity corrected multispectral MRI, *IEEE Trans Med Imaging* **15** (1996), 154–169.

[6] D.L. Pham and J.L. Prince, An adaptive fuzzy C-means algorithm for image segmentation in the presence of intensity inhomogeneities, *Pattern Recognit Lett* **20**(1) (1999), 57–68.

[7] J.C. Bezdek, *Pattern Recognition with Fuzzy Objective Function Algorithms*, New York: Plenum Press, 1981.

[8] Y.A. Tolias and S.M. Panas, On applying spatial constraints in fuzzy image clustering using a fuzzy rule-based system, *IEEE Signal Proc Lett* **5**(10) (1998), 245–247.

[9] Y.A. Tolias and S.M. Panas, Image segmentation by a fuzzy clustering algorithm using adaptive spatially constrained membership functions, *IEEE Trans Syst, Man, Cybernet Part A* **28**(3) (1998), 359–369.

[10] A.W.C. Liew, S.H. Leung and W.H. Lau, Fuzzy image clustering incorporating spatial continuity, *IEE Proc Vis Image Signal Proc* **147**(2) (2000), 185–192.

[11] M.N. Ahmed, S.M. Yamany, N. Mohamed, A.A. Farag and T. Moriarty, A modified fuzzy C-means algorithm for bias field estimation and segmentation of MRI data, *IEEE Trans Med Imaging* **21**(3) (2000), 193–199.

[12] D.L. Pham, *Fuzzy Clustering with Spatial Constraints*, Proceedings of the IEEE International Conference on Image Processing, New York, USA, August, 2002.

[13] S. Chen and D. Zhang, Robust image segmentation using FCM with spatial constraints based on new kernel-induced distance measure, Systems, *Man and Cybernetics, Part B, IEEE Transactions on Volume 34*, Issue 4, Aug. 2004, 1907–1916.

[14] J.-H. Chiang and P.-Y. Hao, A new kernel-based fuzzy clustering approach: support vector clustering with cell growing, *IEEE Transactions on Fuzzy Systems* **11**(4) (Aug 2003), 518–527.

[15] D.-Q. Zhang and S.-C. Chen, Clustering Incomplete Data Using Kernel- Based Fuzzy C-means Algorithm, *Neural Processing Letters* **18**(3) (Dec 2003), 155–162.

[16] J.M. Leski, Fuzzy c-varieties/elliptotypes clustering in reproducing kernel Hilbert space, *Fuzzy Sets and Systems* **141**(2) (2004), 259–280.

[17] E.A. Zanaty, Sultan Aljahdali, Narayan Debnath, *Improving Fuzzy Algorithms for Automatic Magnetic Resonance Image Segmentation*, Proceedings of seventeenth International Conference of Software Engineering and Data Engineering, Los Angeles, California, USA, 2008, pp. 60–66.

[18] M.T. El-Melegy, E.A. Zanaty, Walaa M. Abd-Elhafiez and A. Frag, On cluster validity indexes in fuzzy and hard clustering algorithms for image segmentation, *IEEE International Conference on Computer Vision* **6** VI 5–8, 2007.

[19] D.W. Chakeres and P. Schmalbrock, *Fundamentals of Magnetic Resonance Imaging*, Williams & Wilkins, Baltimore, 1992.

[20] R.B. Buxton, *Introduction to Functional Magnetic Resonance Imaging-Principles and Techniques*, Cambridge University Press, 2002.

[21] A.W.C. Liew and H. Yan, Current methods in the automatic tissue segmentation of 3D Magnetic Resonance Brain Images, *Medical Imaging Reviews* **2** (2006), 91–103.

[22] H. Yan and J.C. Gore, An efficient algorithm for MR image reconstruction without low spatial frequencies, *IEEE Trans Med Imag* **TMI-9** (1990), 179–184.

[23] H. Yan, *Signal Processing in Magnetic Resonance Imaging and Spectroscopy*, Marcel Dekker Inc., 2002.

[24] D.Q. Zhang and S.C. Chen, A novel kernelized fuzzy c-means algorithm with application in medical image segmentation, *Artif Intell Med* **32** (2004), 37–50.

[25] BrainWeb: Simulated brain database, McConnell Brain Imaging Centre, Montreal Neurological Institute, McGill.

[26] D.Q. Zhang and S.C. Chen, A novel kernelized fuzzy C-means algorithm with application in medical image segmentation, *Artificial Intelligent Med* **32** (2000), 37–50.